Available online at www.sciencedirect.com
ScienceDirect
Journal of the European Ceramic Society 29 (2009) 2379–2385
www.elsevier.com/locate/jeurceramsoc

Microstructure and densification of ZrB_2–SiC composites prepared by spark plasma sintering

Ipek Akin [a], Mikinori Hotta [b], Filiz Cinar Sahin [a], Onuralp Yucel [a], Gultekin Goller [a], Takashi Goto [b,*]

[a] *Istanbul Technical University, Metallurgical and Materials Engineering Department, 34469 Maslak, Istanbul, Turkey*
[b] *Tohoku University, Institute for Materials Research, 2-1-1 Katahira, Aoba-ku, Sendai 980-8577, Japan*

Received 3 September 2008; received in revised form 27 December 2008; accepted 13 January 2009
Available online 8 February 2009

Abstract

ZrB_2–SiC composites were prepared by spark plasma sintering (SPS) at temperatures of 1800–2100 °C for 180–300 s under a pressure of 20 MPa and at higher temperatures of above 2100 °C without a holding time under 10 MPa. Densification, microstructure and mechanical properties of ZrB_2–SiC composites were investigated. Fully dense ZrB_2–SiC composites containing 20–60 mass% SiC with a relative density of more than 99% were obtained at 2000 and 2100 °C for 180 s. Below 2120 °C, microstructures consisted of equiaxed ZrB_2 grains with a size of 2–5 μm and α-SiC grains with a size of 2–4 μm. Morphological change from equiaxed to elongated α-SiC grains was observed at higher temperatures. Vickers hardness of ZrB_2–SiC composites increased with increasing sintering temperature and SiC content up to 60 mass%, and ZrB_2–SiC composite containing 60 mass% SiC sintered at 2100 °C for 180 s had the highest value of 26.8 GPa. The highest fracture toughness was observed for ZrB_2–SiC composites containing 50 mass% SiC independent of sintering temperatures.

Keywords: ZrB_2; SiC; Microstructure; Spark plasma sintering; Mechanical properties

1. Introduction

Zirconium diboride (ZrB_2) is a candidate as an ultra-high temperature material because of its high melting temperature (3026.85 °C), high hardness (23 GPa), low theoretical density (6.1 Mg/m^3), high thermal (60–120 W/mK) and electrical ($\sim 10^7$ S/m) conductivity and excellent chemical and physical stability at high temperatures.[1–3]

ZrB_2–SiC composites are known to have higher strength, fracture toughness and oxidation resistance than monolithic ZrB_2, and the addition of SiC particles has been found to improve the oxidation resistance and fracture toughness of ZrB_2.[3,4] ZrB_2–SiC composites have been commonly prepared by using conventional pressureless sintering,[4,5] hot-pressing,[6–13] and reactive hot pressing.[14] However, fully dense composites have been hardly obtained because of high melting temperature and strong covalent bonding of ZrB_2 and SiC.[1–3]

Spark plasma sintering (SPS) makes it possible to densify ZrB_2–SiC composites at a lower temperature and in a shorter time compared with conventional techniques.[1,15–18] In the SPS technique, a pulsed direct current passes through graphite punch rods and dies simultaneously with a uniaxial pressure. Thus, the grain growth can be suppressed by rapid heating and the densification is accelerated at high temperature. Furthermore, the microstructure can be controlled by a fast heating rate and shorter processing times.[15–18]

The number of studies on ultra-high temperature ceramics such as ZrB_2–SiC composites has increased dramatically during the past several years.[15–17] Several experiments have been focused on the production of ZrB_2–SiC composites at low temperatures.[15–19]

In this study, ZrB_2–SiC composites were produced using SPS at different compositions and temperatures,

* Corresponding author.
E-mail address: goto@imr.tohoku.ac.jp (T. Goto).

0955-2219/$ – see front matter © 2009 Elsevier Ltd. All rights reserved.
doi:10.1016/j.jeurceramsoc.2009.01.011

and densification, microstructure and mechanical properties were characterized. The microstructural features of ZrB_2–SiC composites at high temperature were also investigated.

2. Experimental procedure

ZrB_2 (Grade B, H.C. Starck Corp., an average particle size of 2 μm) and α-SiC (Grade UF-10, H.C. Starck Corp., an average particle size of 1 μm) powders were used as starting materials. The powders were weighed in appropriate quantities and mixed in an agate mortar with a small amount of ethanol and then dried. A graphite die 10 mm in inner diameter and 3 mm in thickness was filled with the mixture, followed by sintering using an SPS apparatus (SPS-210LX, SPS Syntex Inc.) at 1800–1900 °C for 300 s and at 2000–2100 °C for 180 s with a heating rate of 1.7 °C/s in a vacuum. A uniaxial pressure of 20 MPa was applied during the entire process. For temperatures above 2100 °C, the temperature of the die was increased at 0.8 °C/s in a vacuum under a pressure of 10 MPa. Pulsed direct current (60 ms/on, 10 ms/off) was applied during the SPS process. The temperature of the die was measured by an optical pyrometer. Linear shrinkage of the specimens during SPS process was continuously monitored by displacement of the punch rods during the process. The effect of thermal expansion of the graphite punch rods with increasing temperature on displacement of the specimens was negligible. The crystalline phases were identified by X-ray diffractometry (XRD; Geigerflex, Rigaku Corp.) in the 2θ range of 10–80° with Cu Kα radiation. The bulk densities of the specimens were determined by the Archimedes' method and converted to relative density using theoretical densities of ZrB_2 (6.1 Mg/m^3) and α-SiC (3.2 Mg/m^3). The polished surfaces of the specimens were observed by scanning electron microscopy (SEM; S-3100H, Hitachi Ltd.). Vickers hardness (H_V) was measured under loads of 0.98–9.8 N and fracture toughness (K_{IC}) was evaluated by a microhardness tester (HM-221, Mitutoyo Corp.). The fracture toughness was calculated from the half-length of a crack formed around the indentations by using the following Eq. (1), where P is load (N) and c is half of the average crack length[20]:

$$K_{IC} = 0.073 \times \left(\frac{P}{c^{1.5}}\right) \quad (1)$$

The average value of the 20 measurements for each sample was used for the evaluations of hardness and toughness. The tensile strength (σ) at room temperature was calculated from the failure load measured using compression test by the following Eq. (2), where P is the failure load (applied diametrically), d is diameter of sample and t is thickness of sample.[21] For the estimation of the tensile strength, one measurement was used for each sample:

$$\sigma = \frac{2P}{\pi dt} \quad (2)$$

3. Results and discussion

3.1. Densification behavior and crystalline phase

The densification of the specimens during SPS process was evaluated by the displacement of punch rods due to shrinkage of the composites. Fig. 1 shows the displacement of ZrB_2 and ZrB_2–SiC composites containing 20–80 mass% SiC at 1400–2000 °C and isothermal shrinkage at 2000 °C for 180 s. The shrinkage of ZrB_2 started at 1825 °C and stopped after holding for 70 s at 2000 °C. The starting temperature of shrinkage for ZrB_2–SiC composites containing 20–60 mass% SiC was significantly lower than that of ZrB_2, and the temperature at which shrinkage of such composites stopped increased with increasing SiC content. Shrinkage of ZrB_2–SiC composites containing 20–60 mass% SiC was completed within 60 s at 2000 °C. For ZrB_2–80 mass% SiC composite, the shrinkage started at 1840 °C and continued after holding at 2000 °C. Thus, the addition of SiC up to 60 mass% to ZrB_2 promoted the shrinkage of ZrB_2–SiC composites. Wang et al.[1] have studied SiC whisker (SiC_w) reinforced ZrB_2 composites prepared by SPS and reported that ZrB_2 started to shrink at about 1200 °C and continued to shrink at a nearly constant rate up to 1550 °C, densification being completed at 1550 °C in 120 s. On the other hand, ZrB_2–SiC_w composites containing 10 vol.% SiC_w began to shrink at 1150 °C, and densification was completed at 1550 °C in 180 s. The density of ZrB_2–SiC_w composites increased with increases in the amount of SiC whiskers. It was concluded that the addition of SiC whiskers to ZrB_2 promoted the densification of composites because SiC can remove the oxygen impurity of the ZrB_2 surface. The removal of the oxygen carrier species from the ZrB_2 surface resulted in an increase in boron activity through the generation of Zr vacancies. This high metal-vacancy concentration would promote lattice diffusion, thus improving densification.[1,8]

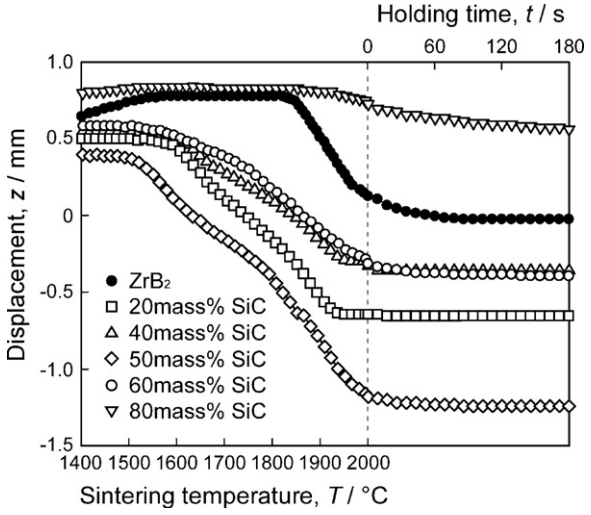

Fig. 1. Effect of sintering temperature on the displacement of ZrB_2 and ZrB_2–SiC composites at 1400 to 2000 °C, and the time dependence of isothermal displacement at 2000 °C up to 180 s.

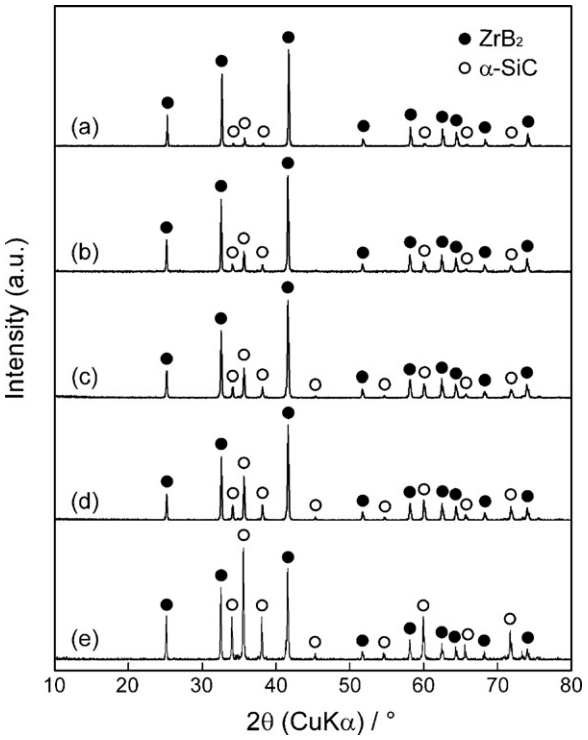

Fig. 2. XRD patterns of ZrB_2–SiC composites containing 20 mass% SiC (a), 40 mass% SiC (b), 50 mass% SiC (c), 60 mass% SiC (d) and 80 mass% SiC (e) sintered at 1800 °C for 300 s.

Fig. 2 shows the XRD patterns of ZrB_2–SiC composites sintered at 1800 °C for 300 s. Characteristic peaks of ZrB_2 and α-SiC were identified and no chemical reaction was detected between ZrB_2 and α-SiC for all compositions at 1800–2100 °C.

The effects of SiC content and sintering temperature on the relative density of ZrB_2–SiC composites are shown in Fig. 3. The relative density of ZrB_2–SiC composites remained below 80% at 1800 °C for 300 s. At 1900 °C for 300 s, the relative density of ZrB_2 was about 80%, while that of ZrB_2–SiC composites containing 20–60 mass% SiC reached 92–95%. The densities of the composites increased with increasing sintering temperature.

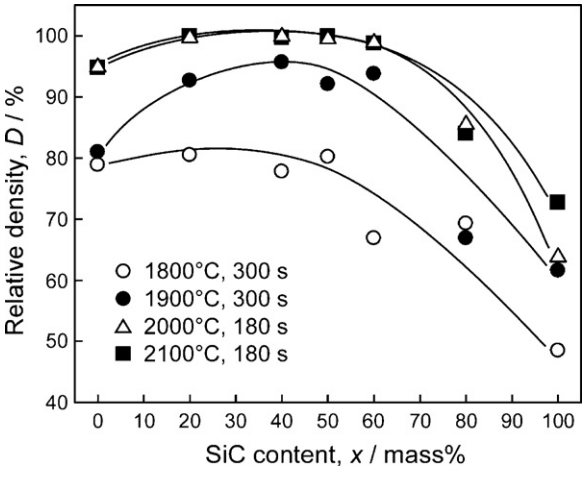

Fig. 3. Effect of SiC content and sintering temperature on relative density of the ZrB_2–SiC composites.

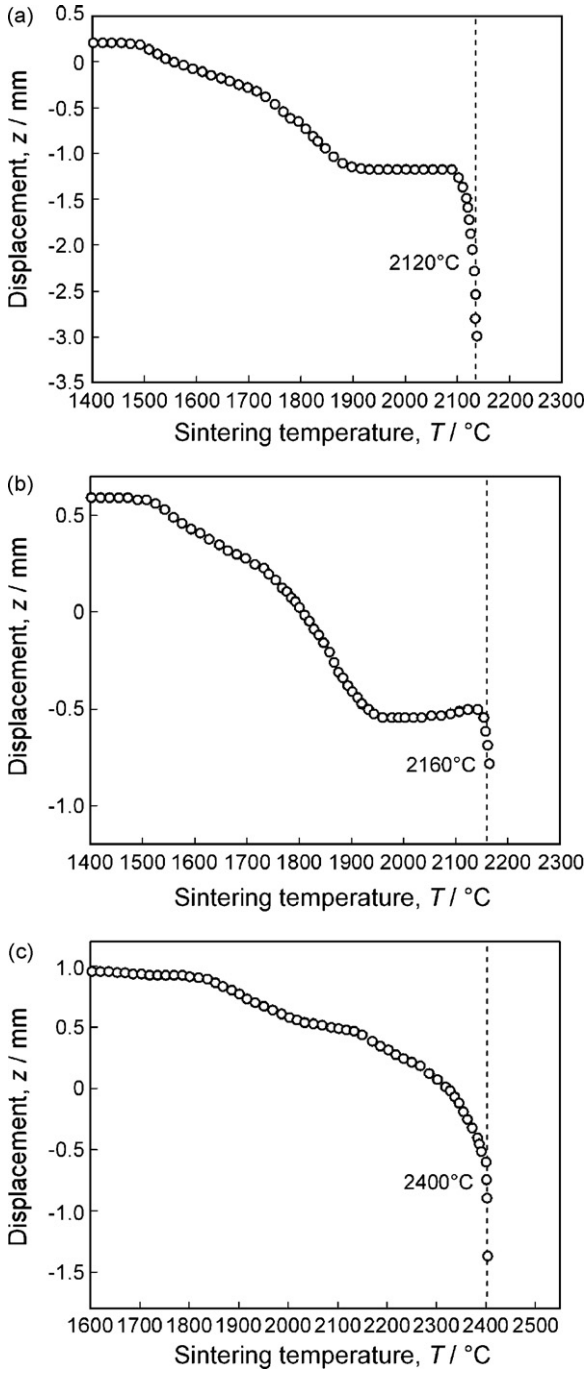

Fig. 4. Relationship between displacement and temperature of ZrB_2–SiC composites containing 40 mass% SiC (a), 50 mass% SiC (b) and 80 mass% SiC (c).

A density of more than 99% was obtained for the composites containing 20–60 mass% SiC sintered at 2000 and 2100 °C for 180 s. The relative densities of the composites sharply decreased at SiC contents of 80 and 100 mass% for sintering temperatures from 1900 to 2100 °C. These results revealed that the addition of SiC up to 60 mass% promoted the densification of ZrB_2–SiC composite, in agreement with the shrinkage results presented in Fig. 1. The densification of the composites at high temperatures may have been facilitated by a eutectic reaction as discussed in the following.

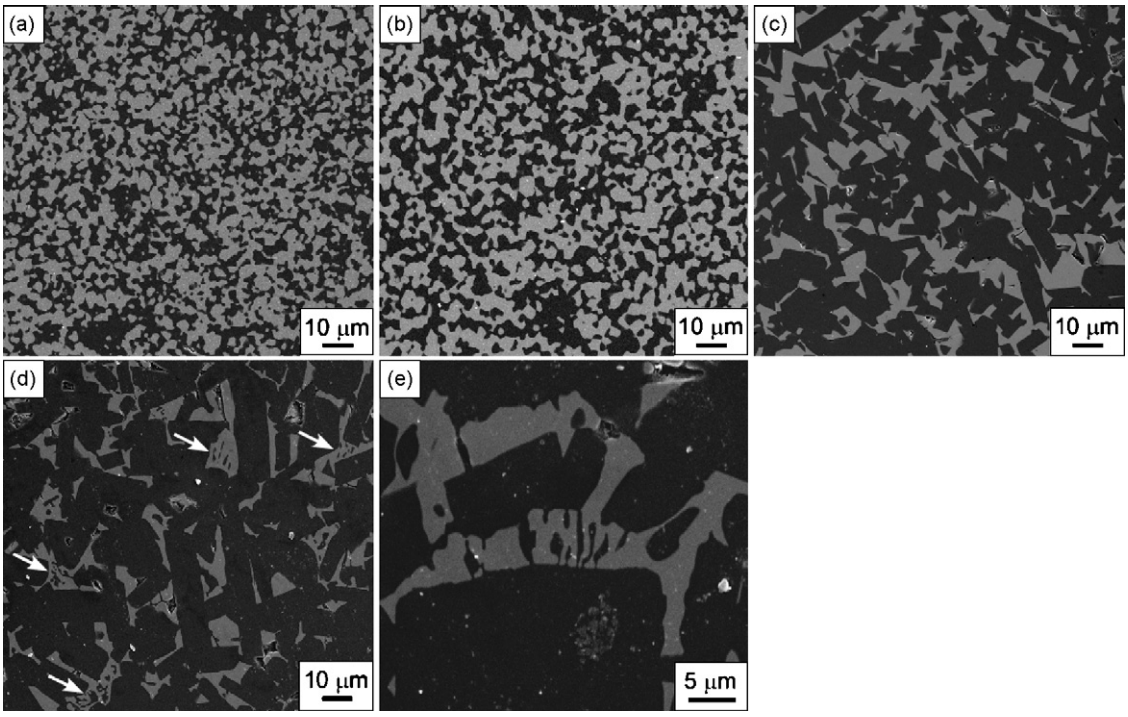

Fig. 5. SEM images of polished surfaces of ZrB_2–SiC composites containing 40 mass% SiC sintered at 1900 °C for 300 s (a), 2100 °C for 180 s (b), 2120 °C (c), 2200 °C (d) without a holding time and high magnification of irregular texture at 2200 °C (e).

3.2. Displacement at high temperature

Fig. 4 shows the relationship between displacements and sintering temperatures of ZrB_2–SiC composites containing 40–80 mass% SiC. For ZrB_2–40 mass% SiC composites, the displacement sharply decreased at 2120 °C because the melted specimen was extruded from the graphite die. Melting temperatures of ZrB_2–SiC composites containing 50 and 80 mass% SiC were apparently higher, 2160 and 2400 °C, respectively. These different melting temperatures could have been caused by the electrical conductivity of ZrB_2 and SiC bodies. In the SPS process, the electrical current passes through the graphite die and/or specimen depending on the electrical conductivity of the specimen. If the specimen is conductive, the electrical current tends to pass through the specimen, and therefore the temperature inside the die becomes higher than that of the die. The sintering temperature was measured from the surface of the die by using a pyrometer. The ZrB_2–SiC system is known as a eutectic system.[3] Although the eutectic temperature has not been precisely determined, it should be independent of composition. Since the electrical conductivity of ZrB_2 is higher than that of SiC, the temperature inside ZrB_2–40 mass% SiC should be higher than that of ZrB_2–80 mass% SiC.[3] The temperature of inside ZrB_2–40 and 50 mass% SiC could be close to 2400 °C, the eutectic temperature of the ZrB_2–SiC system.[3]

3.3. Microstructure

Microstructures of the polished surfaces of ZrB_2–SiC composites containing 40 mass% SiC sintered at 1900–2200 °C are shown in Fig. 5. At 1900 and 2100 °C, the microstructure of the composite consisted of equiaxed ZrB_2 grains (grey) 2–5 μm in size and α-SiC grains (black) 2–4 μm in size. Elongated α-SiC grains (approximately 2–5 μm in width and 5–25 μm in length)

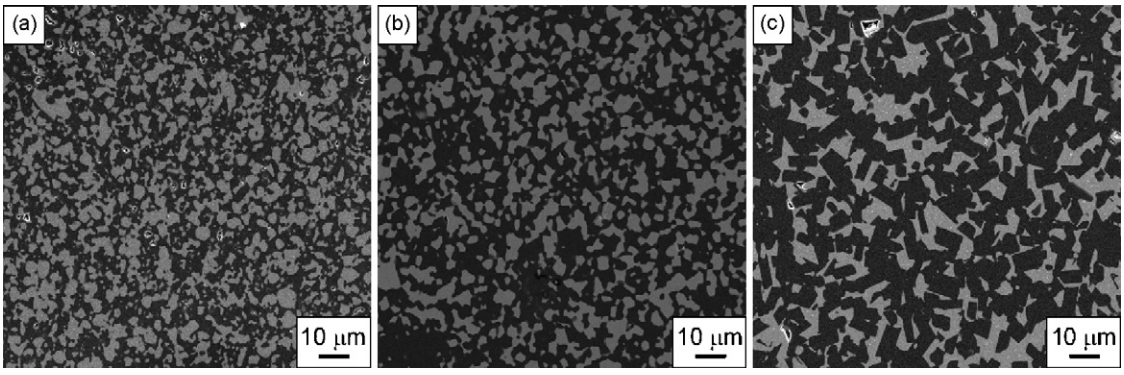

Fig. 6. SEM images of polished surfaces of ZrB_2–SiC composites containing 50 mass% SiC sintered at 1900 °C for 300 s (a), 2100 °C for 180 s (b) and 2165 °C without a holding time (c).

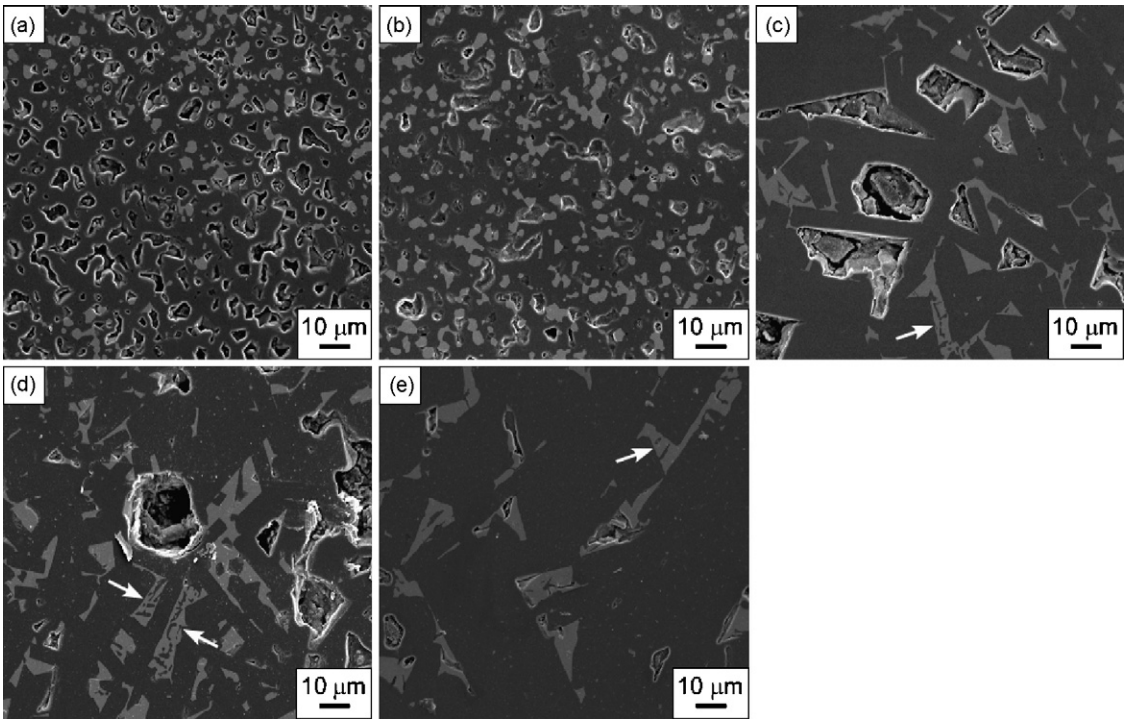

Fig. 7. SEM images of polished surfaces of ZrB_2–SiC composites containing 80 mass% SiC sintered at 2000 °C for 180 s (a), 2100 °C for 180 s (b), 2280 °C (c), 2300 °C (d) and 2360 °C (e) without a holding time.

formed and the edges of ZrB_2 and SiC grains became angular at 2120 °C. At 2200 °C, a laminar texture composed of ZrB_2 and α-SiC grains similar to a eutectic texture was observed as indicated by the white arrows in Fig. 5(d). Fig. 5(e) is a magnified view of the eutectic-like texture in which laminar SiC grains can be seen in ZrB_2 grains. Fig. 6 demonstrates SEM images of the polished surfaces of ZrB_2–SiC composites containing 50 mass% SiC sintered at 1900–2165 °C. At 1900 and 2100 °C, equiaxed ZrB_2 and α-SiC grains were uniformly dispersed in the composites. ZrB_2–SiC composites sintered at 1900 °C for 300 s had a few pores, as shown in Fig. 6(a). At 2165 °C, elongated α-SiC (approximately 1–3 μm in width and 3–6 μm in length) and sharp-edged ZrB_2 and α-SiC grains formed, as shown in Fig. 6(c). The SEM images of polished surfaces of ZrB_2–SiC composites containing 80 mass% SiC are shown in Fig. 7. Fig. 7(a) and (b) clearly shows that the composite containing 80 mass% SiC sintered at 2000 and 2100 °C for 180 s had many pores, in agreement with the relative density data given in Fig. 3. The porous microstructure of ZrB_2–SiC composites at 2000 and 2100 °C could have been caused by difficulty of sintering of SiC grains and difference of thermal expansion coefficient between ZrB_2 and SiC grains.[1] Above 2280 °C, the size of pores increased and elongated α-SiC grains 2–5 μm in width and 10–25 μm in length formed. The decomposition of SiC may have caused the formation of large pores at higher temperatures. At 2280, 2300 and 2360 °C, an abnormally grown texture composed of ZrB_2 and α-SiC grains was detected. We have previously reported a similar eutectic texture in ZrB_2–SiC composites containing 40–80 mol% SiC prepared by arc melting.[3] Therefore, the eutectic-like microstructure suggests that local melting occurs before melting of the whole composite at about 2400 °C as indicated in Fig. 4. The elongated angular α-SiC grains could have been developed in the liquid phase, as frequently observed in liquid phase sintering of α-SiC with metal oxide additives,[22] while the equiaxed microstructure has been obtained through solid-phase sintering, typically using B and C additives.[23]

3.4. Mechanical properties

Fig. 8 demonstrates the effect of SiC content and sintering temperature on the Vickers hardness of ZrB_2–SiC composites at loads of 0.98–9.8 N. ZrB_2–SiC composites had higher hardness

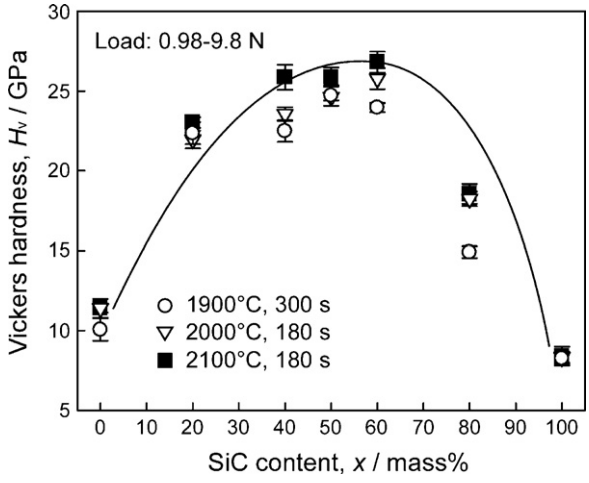

Fig. 8. Effect of SiC content and sintering temperature on the Vickers hardness of ZrB_2–SiC composites sintered at 1900–2100 °C.

than ZrB_2 and SiC monolithic sintered bodies and the hardness of ZrB_2–SiC composites slightly increased with increasing sintering temperature. The hardness of fully dense ZrB_2–SiC composites containing 20–60 mass% SiC sintered at 2000 and 2100 °C reached 26 GPa. The hardness of ZrB_2–SiC composites significantly decreased when SiC content increased from 50 to 80 mass% in the composites. This is attributed to the formation of porous microstructure due to increase in SiC content, as shown in Figs. 3 and 7. Monteverde et al.[7] have prepared a ZrB_2–20 vol.% SiC composite by hot pressing and reported a relative density of 98% and hardness of 14.2 GPa at a load of 9.8 N. Zhu et al.[6] have studied the effect of SiC particle size on the microstructure and the mechanical properties of ZrB_2–30 vol.% SiC composites sintered by hot pressing. They reported a hardness of 17.5–20.7 GPa at a load of 2 N. ZrB_2–30 vol.% SiC composites prepared by hot pressing had a hardness of 20–22 GPa at a load of 2.9 N.[9] Zhao et al.[24] have studied ZrB_2–SiC composites containing 20 to 30 vol.% SiC fabricated by spark plasma sintering-reactive synthesis (SPS-RS). They reported a relative density of 98.5% and hardness of 17 GPa at 9.8 N. This relatively low hardness could be mostly due to an inhomogeneous distribution of SiC. The Vickers hardness of ZrB_2–SiC composites prepared in the present study was higher than those by conventional sintering.

The effects of composition and sintering temperature on the fracture toughness of ZrB_2–SiC composites are depicted in Fig. 9. The fracture toughness of ZrB_2–SiC composites slightly decreased with increasing sintering temperature, and the maximum toughness was obtained for ZrB_2–SiC composites containing 50 mass% SiC for all sintering temperatures. The fracture toughness of ZrB_2 and SiC bodies was 2.5 and 2.1 MPa $m^{1/2}$, respectively. The fracture toughness of ZrB_2–SiC composites containing 50 mass% SiC sintered at 1900 °C for 300 s was 4.1 MPa $m^{1/2}$. This high toughness may have resulted from the fine and uniform microstructure, as shown in Fig. 6. The toughness of ZrB_2–SiC composites containing 10–30 vol.% SiC prepared by hot pressing was 3.9–4.5 MPa $m^{1/2}$,[9,25] while that of ZrB_2–SiC composites containing 20 and 30 vol.% SiC prepared by SPS-RS was 4.3 MPa $m^{1/2}$.[24] These values of toughness are similar to those of the present study. Higher hardness and lower fracture toughness are common in such composites. Although the value of fracture toughness for the present ZrB_2–SiC composites was almost the same as those prepared by conventional sintering such as hot pressing, the hardness was much higher, particularly at high SPS temperature. This might have been due to the self-assembled eutectic microstructure.

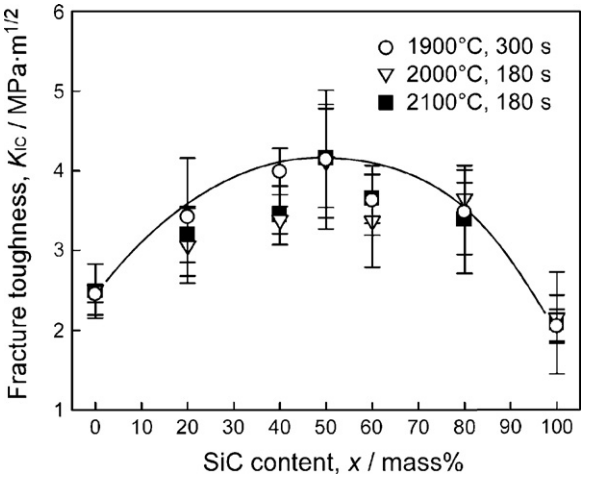

Fig. 9. Effect of SiC content and sintering temperature on the fracture toughness of ZrB_2–SiC composites sintered at 1900–2100 °C.

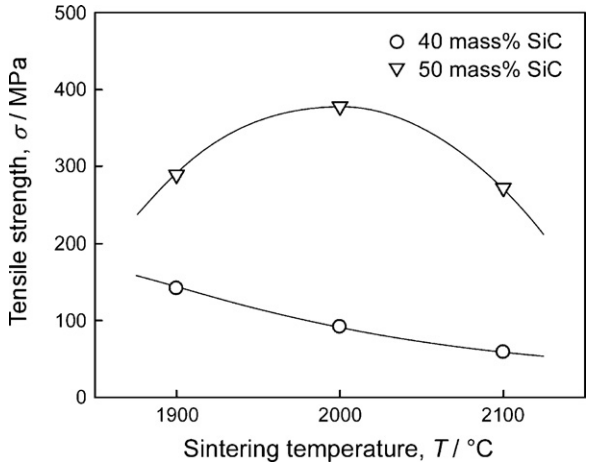

Fig. 10. Effect of sintering temperature on the tensile strength of ZrB_2–SiC composites containing 40 and 50 mass% SiC sintered at 1900–2100 °C.

Fig. 10 shows the effect of sintering temperature on tensile strength of ZrB_2–SiC composites containing 40 and 50 mass% SiC. The tensile strength of ZrB_2–SiC composites containing 50 mass% SiC was higher than that of 40 mass% SiC. This would be attributed to microstructure consisted of finer ZrB_2 and SiC grains in ZrB_2–SiC composites containing 50 mass% SiC. At ZrB_2–SiC composites containing 50 mass% SiC, the tensile strength had a maximum value of 380 MPa at sintering temperature of 2100 °C. This could be due to fully denser composites than that at 1900 °C and finer microstructure than that at 2100 °C.

4. Conclusions

ZrB_2–SiC composites were prepared by SPS at 1800–1900 °C for 300 s, at 2000–2100 °C for 180 s and at higher temperatures without a holding time. The addition of SiC up to 60 mass% improved the densification of ZrB_2–SiC composites. The ZrB_2–SiC composites containing 20–60 mass% SiC sintered at 2000–2100 °C for 180 s reached a maximum relative density of more than 99%. Below 2120 °C, microstructures consisted of equiaxed ZrB_2 grains 2–5 μm in size and α-SiC grains 2–4 μm in size. Elongated α-SiC grains and laminar textures composed of ZrB_2 and fine α-SiC grains formed. ZrB_2 and SiC grains became angular in shape at high temperatures. Vickers hardness of ZrB_2–SiC composites increased with increasing sintering temperature and SiC content up to 60 mass%. ZrB_2–SiC composite with 60 mass% SiC sintered at 2100 °C for 180 s showed the highest value, i.e., 26.8 GPa. The highest fracture toughness, 4.1 MPa $m^{1/2}$, was observed for ZrB_2–50 mass% SiC composites sintered at 1900–2100 °C.

Acknowledgements

This work was supported by the Global COE Program "Materials Integration, Tohoku University," MEXT, Japan and the Rare Metal Substitution Materials Development Project of the New Energy and Industrial Technology Development Organization. The authors thank Dr. H. Kato and Dr. T. Wada (Institute for Materials Research, Tohoku University) for the strength measurement.

References

1. Wang, H., Wang, C., Yao, X. and Fang, D., Processing and mechanical properties of zirconium diboride-based ceramics prepared by spark plasma sintering. *J. Am. Ceram. Soc.*, 2007, **90**, 1992–1997.
2. Tian, W. B., Kan, Y. M., Zhang, G. J. and Wang, P. L., Effect of carbon nanotubes on the properties of ZrB_2–SiC ceramics. *Mater. Sci. Eng. A*, 2008, **487**, 568–573.
3. Tu, R., Hirayama, H. and Goto, T., Preparation of ZrB_2–SiC composites by arc melting and their properties. *J. Ceram. Soc. Jpn.*, 2008, **116**, 431–437.
4. Yan, Y., Zhang, H., Huang, Z., Liu, J. and Jiang, D., *In situ* synthesis of ultrafine ZrB_2–SiC composite powders and the pressureless sintering behaviors. *J. Am. Ceram. Soc.*, 2008, **91**, 1372–1376.
5. Yan, Y., Huang, Z., Dong, S. and Jiang, D., Pressureless sintering of high-density ZrB_2–SiC ceramic composites. *J. Am. Ceram. Soc.*, 2006, **89**, 3589–3592.
6. Zhu, S., Fahrenholtz, W. G. and Hilmas, G. E., Influence of silicon carbide particle size on the microstructure and mechanical properties of zirconium diboride–silicon carbide ceramics. *J. Eur. Ceram. Soc.*, 2007, **27**, 2077–2083.
7. Monteverde, F., Guicciardi, S. and Bellosi, A., Advances in microstructure and mechanical properties of zirconium diboride based ceramics. *Mater. Sci. Eng. A*, 2004, **346**, 310–319.
8. Monteverde, F., Beneficial effects of an ultra-fine α-SiC incorporation on the sinterability and mechanical properties of ZrB_2. *Appl. Phys. A*, 2006, **82**, 329–337.
9. Rezaie, A., Fahrenholtz, W. G. and Hilmas, G. E., Effect of hot pressing time and temperature on the microstrcture and mechanical properties of ZrB_2–SiC. *J. Mater. Sci.*, 2007, **42**, 2735–2744.
10. Zhang, X., Xu, L., Du, S., Han, J., Hu, P. and Han, W., Fabrication and mechanical properties of ZrB_2–SiC_w ceramic matrix composite. *Mater. Lett.*, 2008, **62**, 1058–1060.
11. Rezaie, A., Fahrenholtz, W. G. and Hilmas, G. E., Evolution of structure during the oxidation of zirconium diboride-silicon carbide in air up to 1500 °C. *J. Eur. Ceram. Soc.*, 2007, **27**, 2495–2501.
12. Li, X., Han, J., Zhang, X. and Luo, X., Effect of the rare earth oxides on sintering behavior and micristructure of ZrB_2–SiC ceramics. *Key Eng. Mater.*, 2008, **368–372**, 1740–1742.
13. Hu, P., Zhang, X. H., Han, J. C., Meng, S. H. and Wang, B. L., Microstructure and mechanical properties of SiC whisker-reinforced ZrB_2 ultra-high temperature ceramic. *Key Eng. Mater.*, 2008, **368–372**, 1730–1732.
14. Zimmermann, J. W., Hilmas, G. E., Fahrenholtz, W. G., Monteverde, F. and Bellosi, A., Fabrication and properties of reactively hot pressed ZrB_2–SiC ceramics. *J. Eur. Ceram. Soc.*, 2007, **27**, 2729–2736.
15. Guillard, F., Allemand, A., Lulewicz, J. D. and Galy, J., Densification of SiC by SPS-effects of time, temperature and pressure. *J. Eur. Ceram. Soc.*, 2007, **27**, 2725–2728.
16. Chen, W., Anselmi-Tamburini, U., Garay, J. E., Groza, J. R. and Munir, Z. A., Fundamental investigations on the spark plasma sintering/synthesis process. I. Effect of dc pulsing on reactivity. *Mater. Sci. Eng. A*, 2005, **394**, 132–138.
17. Medri, V., Monteverde, F., Balbo, A. and Bellosi, A., Comparison of ZrB_2–ZrC–SiC composites fabricated by spark plasma sintering and hot pressing. *Adv. Eng. Mater.*, 2005, **7**, 159–163.
18. Bellosi, A., Monteverde, F. and Sciti, D., Fast densification of ultra-high temperature ceramics by spark plasma sintering. *Int. J. Appl. Ceram. Technol.*, 2006, **3**, 32–40.
19. Cao, J., Xu, Q., Zhu, S., Zhao, J. and Wang, F., Microstructure of ZrB_2–SiC composite fabricated by spark plasma sintering. *Key Eng. Mater.*, 2008, **368–372**, 1743–1745.
20. Lawn, B. R. and Fuller, E. R., Equilibrium penny-like cracks in indentation fracture. *J. Mater. Sci.*, 1975, **10**, 2016–2024.
21. *Method of Test for Splitting Tensile Strength of Concrete*, *vol. A-1113*. Japanese Industrial Standards, 1999.
22. Kim, J. Y., Kim, Y. W., Mitomo, M., Zhan, G. D. and Lee, J. G., Microstructure and mechanical properties of α-silicon carbide sintered with yttrium–aluminum garnet and silica. *J. Am. Ceram. Soc.*, 1999, **82**, 441–444.
23. Tanaka, H., In *Silicon Carbide Ceramics-1*, ed. S. Somiya and Y. Inomata. Elsevier Applied Science, New York, 1991, pp. 213–238.
24. Zhao, Y., Wang, L. J., Zhang, G. J., Jiang, W. and Chen, L. D., Preparation and microstructure of a ZrB_2–SiC composite fabricated by the spark plasma sintering-reactive synthesis (SPS-RS) method. *J. Am. Ceram. Soc.*, 2007, **90**, 4040–4042.
25. Chamberlain, A. L., Fahrenholtz, W. G., Hilmas, G. E. and Ellerby, D. T., High-strength zirconium diboride-based ceramics. *J. Am. Ceram. Soc.*, 2004, **87**, 1170–1172.